MINIREVIEW

Natural and amyloid self-assembly of S100 proteins: structural basis of functional diversity

Günter Fritz[1], Hugo M. Botelho[2], Ludmilla A. Morozova-Roche[3] and Cláudio M. Gomes[2]

1 Department of Neuropathology, University of Freiburg, Germany
2 Instituto de Tecnologia Química e Biológica, Universidade Nova de Lisboa, Oeiras, Portugal
3 Department of Medical Biochemistry and Biophysics, Umeå University, Sweden

Keywords
amyloid; fibril; function; metal ions; misfolding; oligomer; self-assembly; structure; S100 proteins

Correspondence
C. M. Gomes, Instituto de Tecnologia Química e Biológica, Universidade Nova de Lisboa, Oeiras, Portugal
Fax: +351 214 411 277
Tel: +351 214 469 332
E-mail: gomes@itqb.unl.pt
L. A. Morozova-Roche, Department of Medical Biochemistry and Biophysics, Umeå University, Umeå, Sweden
Fax: +46 90 786 9795
Tel: +46 90 786 5283
E-mail: ludmilla.morozova-roche@medchem.umu.se

(Received 27 May 2010, revised 2 August 2010, accepted 18 August 2010)

doi:10.1111/j.1742-4658.2010.07887.x

The S100 proteins are 10–12 kDa EF-hand proteins that act as central regulators in a multitude of cellular processes including cell survival, proliferation, differentiation and motility. Consequently, many S100 proteins are implicated and display marked changes in their expression levels in many types of cancer, neurodegenerative disorders, inflammatory and autoimmune diseases. The structure and function of S100 proteins are modulated by metal ions via Ca^{2+} binding through EF-hand motifs and binding of Zn^{2+} and Cu^{2+} at additional sites, usually at the homodimer interfaces. Ca^{2+} binding modulates S100 conformational opening and thus promotes and affects the interaction with p53, the receptor for advanced glycation endproducts and Toll-like receptor 4, among many others. Structural plasticity also occurs at the quaternary level, where several S100 proteins self-assemble into multiple oligomeric states, many being functionally relevant. Recently, we have found that the S100A8/A9 proteins are involved in amyloidogenic processes in corpora amylacea of prostate cancer patients, and undergo metal-mediated amyloid oligomerization and fibrillation *in vitro*. Here we review the unique chemical and structural properties of S100 proteins that underlie the conformational changes resulting in their oligomerization upon metal ion binding and ultimately in functional control. The possibility that S100 proteins have intrinsic amyloid-forming capacity is also addressed, as well as the hypothesis that amyloid self-assemblies may, under particular physiological conditions, affect the S100 functions within the cellular milieu.

Introduction

The S100 protein family represents the largest subgroup within the Ca^{2+}-binding EF-hand superfamily. The name of the protein family has derived from the fact that the first identified S100 proteins were obtained from the soluble (S) bovine brain fraction upon fractionation with saturated (100%) ammonium sulfate [1]. The genes encoding the large majority of human S100 proteins are organized in a gene cluster located in chromosomal region 1q21 [2,3]. This region harbours the genes of S100A1 to S100A16, which are the result of several gene duplication events. The genes of other S100 proteins, such as S100B, S100P or S100Z, are located in humans in chromosomes 21, 4 and 5, respectively.

Abbreviations
RAGE, receptor for advanced glycation endproducts; ThT, thioflavin-T.

In humans, 21 different S100 proteins have been identified to date and similar numbers have been found in other mammalia based on genomic analysis. Further diverse branches of S100 proteins were found in other vertebrates. The level of sequence identity among the S100 proteins within one species varies considerably, e.g. for human proteins the identity ranges between 22% and 57%. Many S100 proteins exhibit very distinctive expression patterns in different tissues and cell types, as well as specific subcellular localization, underlining the high degree of specialization among them. Corresponding to their diversity in primary structure and localization, the S100 proteins are involved in the regulation of a multitude of cellular processes, such as cell cycle control, cell growth, differentiation and motility. Considering the diverse S100 protein functions, it is no surprise to find that these proteins are implicated in numerous human diseases, such as different types of cancer characterized by altered expression levels of S100 proteins [4], neurodegenerative disorders such as Alzheimer's disease [5,6], inflammatory and autoimmune diseases [4].

The conformational properties and function of S100 proteins are modulated by metal ion binding. The binding of Ca^{2+} to EF-hand type domains triggers conformational changes allowing interactions with other proteins. In many S100 proteins, additional binding of Zn^{2+} fine tunes protein folding and function [7,8]. Intracellularly, S100 proteins act as Ca^{2+} sensors, translating intracellular Ca^{2+} level increases into a cellular response. An increasing number of S100 proteins is also reported to occur extracellularly, binding to the receptor for advanced glycation endproducts (RAGE) [9–12] or Toll-like receptor 4 [13]. Recently, a new property among S100 proteins was unveiled: we have found that the S100A8/A9 proteins can form amyloids in a metal ion-mediated fibrillation process in the ageing prostate [14]. In the following sections these aspects and the possible functional and biological implications of physiological amyloid formation by S100 proteins will be addressed.

Structural properties of S100 proteins

Monomers, dimers and multimers

Most S100 protein family members form homo- and heterodimers, but with largely different preferences. Larger multimeric assemblies, such as tetramers [11,15,16], hexamers [11,17,18] and octamers [11], also form spontaneously. The exception is S100G, which functions as a monomer. Other S100 proteins might exist as monomers at very low concentrations in the cell [19]. The monomer–dimer equilibrium may facilitate heterodimer formation in the cell [19,20]. Several heterodimeric S100 proteins have been reported, but only the S100A8/A9 heterodimer is well characterized [13,16,21–23]. The list of S100 heterodimers is steadily growing: S100B forms heterodimers with S100A1 [24], S100A6 [25,26] and S100A11 [26]; S100A1 with S100A4 [27] and S100P [28]; and S100A7 with S100A10 [29]. Noncovalent multimers were observed for S100A12 [18], S100A8/A9 [16,30], S100B [11], S100A4 [31] and a Zn^{2+}-dependent tetramer for S100A2 [15]. Comparison of the structure of S100A8/A9 with those of the corresponding homodimers revealed that the solvent exposed area is reduced in the heterodimer, which might represent the driving force of heterodimer formation [16]. It is proposed that heterodimer formation apart from homodimeric assembly might lead to further diversification of S100 protein functions [20,32].

EF-hand Ca^{2+} binding

All S100 proteins exhibit the same key structural features. Each S100 monomer is $\sim$ 10–12 kDa and composed of two EF-hand helix-loop-helix structural motifs arranged in a back to back manner and connected by a flexible linker. The C-terminal EF-hand contains the classical Ca^{2+}-binding motif, common to all EF-hand proteins. The loop has a typical sequence signature of 12 amino acids flanked by helices H_{III} and H_{IV} (Fig. 1B). The N-terminal EF-hand exhibits a slightly different architecture and contains a specific 14 amino acid motif flanked by helices H_I and H_{II} (Fig. 1A). This motif is characteristic for S100 proteins and therefore it is often called 'S100-specific'or 'pseudo EF-hand'. Generally, the dimeric S100 proteins bind four Ca^{2+} ions per dimer with micromolar to hundreds micromolar binding constants and strong cooperativity. The S100 protein dimer interface is formed by helices H_I and H_{IV} from both monomers, building a compact four helix bundle (Fig. 1C,D).

Zn^{2+}-binding sites

Many S100 proteins are reported to bind Zn^{2+} with high affinity. The Zn^{2+}-binding S100 proteins can be subdivided into two subgroups: one, where Cys residues are involved in Zn^{2+} coordination, and a second group, where Zn^{2+} binds exclusively via the side chains of His, Glu and Asp residues. The first group has been characterized by spectroscopic analysis in combination with molecular modelling, showing, for example for S100A2 that Zn^{2+} is coordinated by

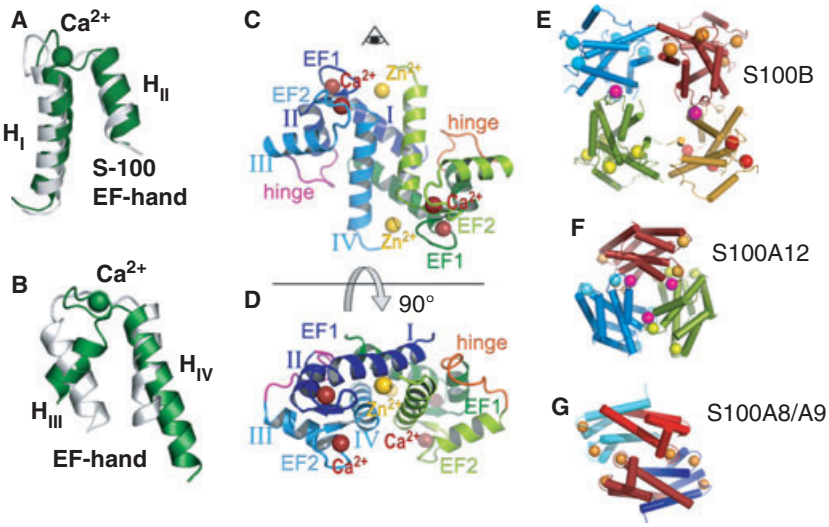

Fig. 1. Structure of S100 proteins. (A,B) Calcium-driven conformational changes at the EF-hands in S100 proteins. Structure of the N-terminal, S100-specific EF-hand (A) and the C-terminal, canonical EF-hand (B) in the metal-free (lighter) and Ca^{2+}-bound (darker) form of S100A6. The EF-hand flanking helices (H_I–H_{IV}) are identified. (C,D) Structure of the human S100B homodimer loaded with Ca^{2+} and Zn^{2+} (T. Ostendorp, J. Diez, C.W. Heizmann, G. Fritz, unpublished results, 3D10). (C) Side view; (D) top view. The monomers are shown in blue and green. The N-terminal S100-specific EF-hand (EF-hand 1) is shown in a dark colour, the C-terminal canonical EF-hand in a brighter colour (EF-hand 2). The hinges connecting both EF-hands are shown in magenta and orange. The four bound Ca^{2+} ions are shown as red spheres. The two Zn^{2+} bound at the dimer interface of S100B are shown as yellow spheres. (E–G) Multimeric states of S100 proteins. S100B octamer, 2H61 (E), S100A12 hexamer, 1GQM (F) and S100A8/A9 tetramer, 1XK4 (G). Each dimer in S100B or S100A12 is shown in an individual colour. S100A8 is shown in red, S100A9 in blue. Bound Ca^{2+} ions are shown as spheres; intersubunit Ca^{2+} ions are shown as magenta spheres.

residues from different monomers [15]. For the second group, encompassing S100A7, S100A8/A9, S100A12 and S100B, detailed structural information mainly by X-ray crystallography is available. S100A7, S100A12 and S100B bind two Zn^{2+} ions per homodimer at the subunit interface that further stabilize the dimer [17,33,34].

Metal ions as modulators of S100 conformation and stability

The metal-binding properties of S100 proteins have a pivotal influence as modulators of their conformation, folding, oligomerization state and, ultimately, function. As outlined above, S100 proteins are able to bind different metal ions, including Ca^{2+}, Zn^{2+} and Cu^{2+}. In the Ca^{2+}-free state, the helices of both EF-hands in each monomer adopt an antiparallel conformation masking the target protein interaction site. Upon Ca^{2+} binding, the C-terminus undergoes a major conformational change (Fig. 1B). Helix H_{III} makes a 90° movement, opening the structure, whereas the N-terminal EF-hand exhibits only minor structural changes (Fig. 1A,B). This leads to the exposure of a wide hydrophobic cleft, which mediates target recognition. This surface is formed by residues of the hinge region, helix H_{III} and the C-terminus, the regions exhibiting the largest variation in amino acid sequence throughout the S100 family. Helices H_I and H_{IV} barely move during Ca^{2+} binding, maintaining the dimeric state of the S100 proteins. The residue invariability and the conserved spatial arrangement of the helices at the dimer interface are the basis for heterodimer formation. In the absence of Ca^{2+}, the EF-hands can accommodate Na^+ (as in S100A2 [35]) or Mg^{2+} ions. The reported affinities for Mg^{2+} ions are rather low, having only a minor effect on Ca^{2+} binding.

In addition to Ca^{2+}, many S100 proteins (S100B, S100A2, S100A3, S100A6, S100A7, S100A8/9, S100A12) bind Zn^{2+} in specific sites, whose metallation state also influences protein conformation, folding and presumably function. One of these proteins is S100A7, which is upregulated in the keratinocytes of patients suffering from the chronic skin disease psoriasis, and which has been hypothesized to account for the microbial resistance of skin [36]. The structure of this protein has elicited two identical high-affinity Zn^{2+}-binding sites formed by His/Asp residues from different monomers that 'clip' together the two subunits. A substantial stabilization of the dimer is expected to arise from Zn^{2+} binding, as it promotes head-to-tail interactions between the two monomers, although in

this particular case Zn^{2+} does not seem to be essential for protein stability [33].

There is evidence for an interesting cross-talk between Ca^{2+} and Zn^{2+} binding to S100 proteins, illustrating how binding of different metal ions results in conformational adjustments and modulation of protein folding and function. In S100B and S100A12, Zn^{2+} binding leads to an increase in Ca^{2+} affinity [37,38], whereas in S100A2 the opposite effect was observed, i.e. Zn^{2+} decreased Ca^{2+} affinity, pointing to an interplay of the metal ions in the activation of S100 proteins [15]. For S100A12 and S100B, the molecular mechanism of the increase in Ca^{2+} affinity by Zn^{2+} can be deduced from the structural information available (T. Ostendorp, J. Diez, C.W. Heizmann, G. Fritz, unpublished results) [17]. In both proteins there is one Zn^{2+} coordinating His residue located in the Ca^{2+}-binding loop, which might help to stabilize the Ca^{2+}-bound conformation, thereby increasing Ca^{2+} affinity. The structure of S100A12 with only bound Zn^{2+} also shows that Zn^{2+} alone can already induce structural changes similar to those induced by Ca^{2+}, which will also lead to an increase in Ca^{2+} affinity. Other Zn^{2+} coordinating residues are located in the C-terminus of the S100 proteins. Zn^{2+} coordination leads to a stabilization and extension of the C-terminal helix, changing the orientation of residues involved in target binding. As expected from these structural changes, Zn^{2+} binding modulates target binding properties of different S100 proteins. For example, Zn^{2+} prevents S100A8/A9 binding to arachidonic acid [39]. On the other hand, Zn^{2+} and Ca^{2+} binding to S100A9 are both required for interaction with receptors such as RAGE or Toll-like receptor 4 [9,13]. Similarly, Zn^{2+} increased the Ca^{2+}-dependent interaction of S100A12 with RAGE [40]. In the case of S100B, Zn^{2+} alone could trigger binding to tau [41,42] or IQGAP1 [43]. Moreover, Zn^{2+} binding enhanced the Ca^{2+}-dependent interaction with AHNAK [44] and the target protein-derived peptide TRTK-12 [45].

Recent work on the S100A2 protein, a cell cycle regulator that binds and activates p53 in a Ca^{2+}-dependent manner, has shown that metal ion binding influences protein conformation and stability [7]. S100A2 binds two Ca^{2+} and two Zn^{2+} ions per subunit, known to be associated with activation (Ca^{2+}) or inhibition (Zn^{2+}) of downstream signalling. Zn^{2+} binds at distinct sites that have different metal-binding affinities, and physiologically relevant Zn^{2+} concentrations decrease the affinity for Ca^{2+} binding, resulting in a blockage of p53 activation. It has been recently elicited that the S100A2 conformation is sensitive to the metallation state, although rearrangements resulting from metal binding preserve the overall fold of the protein: S100A2 is destabilized by Zn^{2+} and stabilized by Ca^{2+}, suggesting a synergistic effect between the binding of different metals. Thus, the decrease in Ca^{2+} affinity through Zn^{2+} is presumably a result of the general destabilization of the protein. Further contributions might come from the exposure of a hydrophobic surface upon Zn^{2+} binding, making additional exposure of the hydrophobic surface induced by Ca^{2+} less favourable. The antagonistic effect of Zn^{2+} and Ca^{2+} in the control of S100A2 stability provides a molecular rationale for the action of both metal ions: hypothetically, in tissues expressing S100A2, the Zn^{2+} imbalance, which may arise in some types of cancer as a result of the upregulation of Zn^{2+} transporters [46,47], may contribute to enhanced cell proliferation through destabilization of S100A2. This would impair the interaction with p53 and disrupt subsequent downstream cell cycle regulation. This further illustrates how the binding of different metal ions to S100 proteins has the potential to result in conformational adjustments and modulation of protein folding and functions.

A number of S100 proteins also bind Cu^{2+} (S100B [48], S100A5 [49], S100A12 [50] and S100A13 [51]) and this frequently occurs at the same sites to which Zn^{2+} binds. That is, for example, the case in S100A12, an important protein in the inflammatory response and a factor in host/parasite defences, which binds Cu^{2+} and Zn^{2+} at the same site and corresponds to the Zn^{2+}-binding site in S100A7, evoking a possibly similar structural and functional role. S100B, one of the most abundant proteins in the human brain, also binds Cu^{2+}, and in this case a putative neuroprotective role was suggested.

S100 functional oligomers

Metal ions also play a crucial role in the formation of larger oligomeric species of S100 proteins, namely tetramers, hexamers and octamers. These are, in many cases, essential for biological function and signalling: tetrameric S100B [11] and hexameric S100A12 [52] bind RAGE with higher affinity than the dimeric counterparts, only multimeric S100A4 promotes neurite outgrowth [53], and microtubule formation is only promoted by the Ca^{2+}-induced S100A8/A9 tetramer [16]. Ca^{2+}-loaded S100A12 forms a functional hexamer whose quaternary structure is maintained by additional interdimer bridging Ca^{2+} ions, which are coordinated by residues from the C-terminal EF-hand and helix H_{III} from two adjacent dimers. This arrangement of ligands for the interdimer Ca^{2+} 'cross-linker' is only possible when the C-terminal EF-hand is in the

Ca^{2+}-bound state [50]. Similarly, two S100A8/A9 heterodimers can assemble into a heterotetramer in a strictly Ca^{2+}-dependent manner [16]. However, the initial S100A8/A9 heterodimer can be formed in the presence or absence of Ca^{2+}. By contrast, the formation of S100B tetramers is not dependent on Ca^{2+} and the tetramer remains stable in the absence of the metal ion [11]. This difference may result from the additional hydrophobic moieties found in interfaces of S100B, which are essentially polar in S100A12 and S100A8/A9 [11]. Nevertheless, the presence of Ca^{2+} enhances the oligomerization of S100B into hexamers and octamers, and the octameric crystal structure reveals intersubunit Ca^{2+} ions. The oligomerization role is not restricted to Ca^{2+}, as in S100A2 binding of Zn^{2+} to the low affinity site triggers the formation of a tetramer via the assembly of two S100A2 dimers [15]. Together, these results point to a very clear role of metal ions in the formation of functional S100 oligomers. However, novel roles for non-functional S100 oligomers are emerging with the recent finding of metal-dependent amyloid formation by S100A8/A9, which will be addressed further.

Functional diversity of S100 proteins

To date a great number of distinct functions have been attributed to S100 proteins in both the intra- and extracellular milieu. Although S100 proteins appear to lack enzymatic activity themselves, they play biological roles through binding to other proteins and changing the activity of their targets. As discussed above, the conformation and even oligomerization state of S100s are responsive to Ca^{2+} and consequently they mediate Ca^{2+} signals by binding to other intracellular target proteins and modulating their conformation and activity in a Ca^{2+}- and possibly also in a Zn^{2+}- and Cu^{2+}-dependent manner. Indeed, the assembly into multiple complexes is considered in general as a significant generic mechanism of protein functional diversification via varying their conformational states and associated ligands [54]. Several S100 proteins exhibit Ca^{2+}-dependent interactions with metabolic enzymes (S100A1 and S100B with aldolase C) [55], with kinases (S100B with Ndr or Src kinases) [56,57], with cytoskeletal proteins (S100A1 with tubulin, S100B with CapZ and S100P with ezrin) [58–63] or with DNA-binding proteins (S100A2, S100A4 and S100B interact with p53) [64–66]. As a result, intracellularly S100 proteins are involved in the regulation of the cell cycle, cell growth and differentiation, apoptosis, migration, calcium homeostasis, protein phosphorylation, cellular motility and other important processes.

Some S100 proteins, including S100A4, S100A7, S100A8/A9, S100A11, S100A12, S100B and others, can be secreted, exhibiting cytokine-like and chemotactic activity. When S100A7, S100A8, S100A9, S100A12 or S100B are secreted in response to cell damage or activation, they become danger signals, activating other immune and endothelial cells. Accordingly, they were defined as damage-associated molecular pattern molecules in innate immunity [67,68]. The S100A8/A9 complex accounts for up to 40% of total cytosolic proteins in neutrophils and secreted S100A8/A9 as well as S100A12 are found at high concentrations in inflamed tissues, producing strong proinflammatory effects. S100A8 and S100A9 activate Toll-like receptor 4, acting as innate amplifiers of inflammation and cancer [69,70], with direct implication in metastasization [70]. Recently it was demonstrated in a mouse model that via activation of Toll-like receptor 4, S100A8 and S100A9 induce the development of systemic autoimmunity [69].

S100B is highly expressed in the human brain and actively secreted by astrocytes, neurons, microglia, glioblastoma or Schwann cells [71]. Its extracellular concentration reaches micromolar levels after traumatic brain injury and in neurodegenerative disorders such as Alzheimer's disease or Down's syndrome. The action of S100B is strongly dependent on its concentration: at nanomolar levels it is neuroprotective, whereas in the micromolar concentration range it promotes apoptosis [72]. Both trophic and toxic effects of extracellular S100B are mediated by RAGE [23]. A large number of S100 proteins have been shown to interact with RAGE, including S100A1, S100A2, S100A4, S100A5, S100A6, 100A7, S100A8/A9, S100A11, S100A12 and S100B [22]. However, S100-associated cell signalling may be promiscuous. This can be best exemplified through S100A8/A9, which promotes RAGE-dependent cell survival [73] as well as multiple RAGE-independent cell death pathways [74–76].

Because of their deregulated expression, response to stress and association with neoplastic, degenerative and autoimmune disorders, S100 proteins gain significant interest as potential therapeutic targets. In view of the large number of tertiary and quaternary structures adopted by S100s and the complex structure–functional relationship affecting their interactions with target proteins, it is tempting to speculate that this variability may account for the promiscuity of S100 proteins. Therefore, systematic studies of the conformational changes and oligomerization of S100 proteins will be of critical importance in the development of potential therapeutics.

Amyloid formation by S100A8/A9 proteins

Recently, we have found a new amyloidogenic property of S100A8/A9 proteins, implicating them in another degenerative process in the ageing prostate, specifically in amyloid deposition and tissue remodelling [14]. The conversion of functional proteins and peptides into insoluble amyloid structures and their deposition in a variety of tissues and organs is a hallmark of a growing number of age-related degenerative disorders, including Alzheimer's and Parkinson's diseases, type II diabetes and systemic amyloidoses. Prostate amyloid deposits known as corpora amylacea belong to a type of localized amyloidoses, they are associated with age-related prostate tissue remodelling and occur frequently in middle-aged and elderly men.

These inclusions can vary in size from submillimetre to a few millimetres in diameter (Fig. 2A) and can, in some instances, constitute up to a third of the prostate gland bulk weight. Despite their high prevalence in later life [77], their role in prostate benign and malignant changes is still disputed. The fact that proinflammatory S100 proteins contribute to corpora amylacea formation elevates their role as potential cancer risk factors. There is a growing body of evidence indicating that inflammation is a crucial prerequisite in prostate pathogenesis, as it is found to be associated with 40–90% of benign prostatic hyperplasia and with 20% of all human cancers [78]. Prostate cancer is the most common noncutaneous malignant neoplasm in men in Western countries, affecting several million men in the Western world, and its incidence is rising rapidly with population ageing. Therefore, cancer risk assessment is of critical significance in its preventing strategies.

By using mass spectrometry, gel electrophoresis and western blot analyses, we have found that proinflammatory S100A8/A9 proteins are persistently present in all specimens obtained as a result of prostatectomy in prostate cancer patients [14]. Immunohistochemical

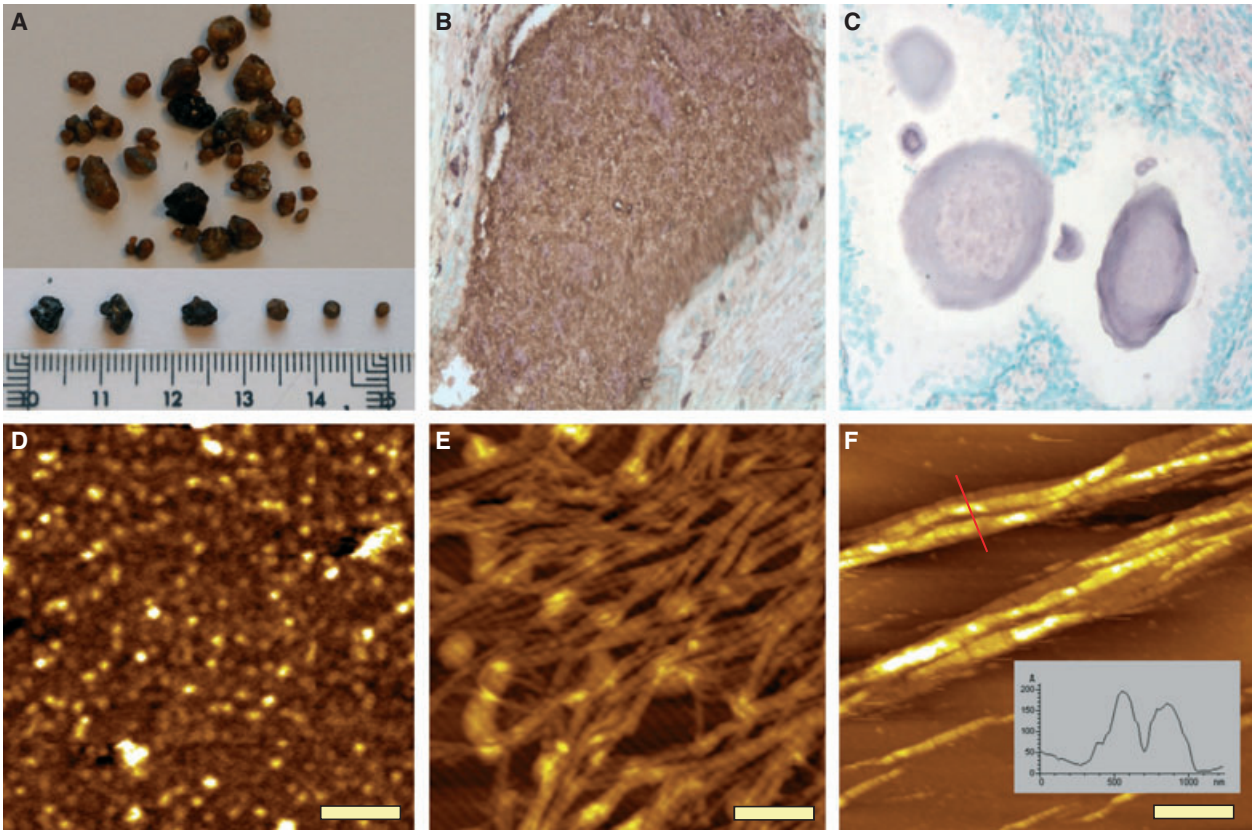

Fig. 2. Amyloid formation by S100A8/A9 proteins in the ageing prostate. (A) Corpora amylacea deposits extracted as a result of prostatectomy (ruler is shown in centimetres). (B) Co-immunostaining of corpora amylacea with anti-S100A8 (shown in purple) and anti-S100A9 IgG (shown in brown). (C) Immunostaining of corpora amylacea by antibodies towards amyloid fibrils (shown in purple). Atomic force microscopy images of (D) *ex vivo* amyloid oligomers; (E) *ex vivo* amyloid fibrillar network and (F) amyloid fibrils produced *in vitro* at pH 7.4, 37 °C with agitation. The fibril height analysis corresponds to the cross-section marked as a red line. Scale bars represent 250 nm.

analysis of corpora amylacea revealed that they are stained positively with both anti-S100A8 and anti-S100A9 IgGs (Fig. 2B). Positive foci of S100A8 and S100A9, including glandular epithelial cells and tissue macrophages, were observed in the tissues adjacent to corpora amylacea inclusions, indicating that the latter infiltrate inflamed glands and ultimately lead to raising local concentrations of S100A8/A9. Proteinaceous compounds constitute up to 30–40% of corpora amylacea deposits, as revealed by X-ray photoelectron spectroscopy and FTIR, whereas the rest correspond to inorganic components consisting of hydroxylapatite [$Ca_5(PO4)_3OH$] and whitlockite [$Ca_2(PO4)_3$], containing high concentrations of Zn^{2+} ions. The calcification of protein deposits leads effectively to their further stabilization in the protease-rich prostate fluid. The mineral content of corpora amylacea was rather uniform in all seven studied patients, indicating that calcification can be a regulated process. A recently reported function of S100A9 is associated with promoting calcification [79], suggesting that dystrophic calcification of corpora amylacea deposits could be influenced by the activities of S100A8/A9.

Remarkably, all corpora amylacea specimens were also stained with anti-amyloid fibril IgGs [80] (Fig. 2C) and Congo Red dye, used as a marker for the presence of the amyloid form of proteins, demonstrating that the amyloid material constitutes a significant mass of these specimens. Indeed, atomic force and transmission electron microscopy analyses revealed a variety of highly heterogeneous aggregates in the corpora amylacea extracts (Fig. 2D, E), ranging from oligomeric species to extensive networks of mature fibrils, which is typical for the amyloid assemblies [81], as well as larger-scale supramolecular assemblies, reaching a few microns in length. Similar amyloid forms of S100A8/A9 were produced *in vitro*, providing further insight into their amyloidogenic properties. The S100A8/A9 complexes, extracted from granulocytes and produced recombinantly from *Escherichia coli*, were each incubated under the native conditions of pH 7.4 and 37 °C with agitation and at pH 2.0 and 57 °C without agitation. Under both conditions, the proteins were assembled into heterogeneous fibrillar species. At pH 7.4, species resembling *ex vivo* oligomers and short protofilaments were formed after 2 weeks and thick bundles of fibrils with heights of 15–20 nm and a few microns in length constituted the major population of fibrillar aggregates after 8 weeks of incubation (Fig. 2F). In the S100A8/A9 samples incubated at pH 2.0, oligomeric species and protofilaments also emerged in 2 weeks, while after 4 weeks of incubation flexible fibrils with a height of $\sim$ 4–5 nm and microns in length together with straight and rigid fibrillar structures a few hundred nanometres long were observed, all closely resembling the *ex vivo* species.

It is important to note that Ca^{2+} and Zn^{2+} play a critical role in promoting amyloid assembly of S100A8/A9 proteins. As *ex vivo* corpora amylacea deposits are calcified and contain zinc salts, these ions can play a critical role in S100A8/A9 amyloid formation *in vivo*. Indeed, after 2 weeks of incubation, the S100A8/A9 amyloid protofilaments of $\sim$ 2 nm height were assembled in the presence of 10 mM $ZnCl_2$ and in a suspension of $Ca_3(PO_4)_2$ [14], but not when EDTA was added in solution. These species were converted into the fibrillar assemblies after 4 weeks of incubation, and again no filamentous structures developed in the presence of EDTA.

The bundles of amyloid fibrils of S100A8/A9 proteins, formed both *in vivo* and *in vitro* (Fig. 2F), are among the largest reported amyloid supramolecular species. The lateral association and thickening of the fibrils is probably a contributing factor to their stability in the prostate gland. It has been suggested that the various functions of the S100A8/A9 hetero- and homo-oligomers may be regulated by their differential protease sensitivity [22]. The hetero-oligomeric complexes of S100A8/A9 are characterized by significant stability and protease resistance comparable with that of prions. In the protease-rich environment of the prostate gland, and especially at sites of inflammation, where proteases are present at even higher levels, protease resistance of the S100A8/A9 proteins could favour their accumulation and conversion into amyloid structures. If so, the amyloid structures formed by S100A8/A9 can be at the extreme end of the scale of resistance to proteolysis.

As prostatic fluid is very rich in protein content, small quantities of other proteins were also found in the corpora amylacea inclusions, presumably being trapped in the aggregating and growing deposits. Among them, the finding of *E. coli* DNA and *E. coli* proteins indicates that corpora amylacea formation may be associated with bacterial infection, consequently causing inflammation in surrounding tissues during the course of corpora amylacea establishment and growth. The identification of the highly amyloidogenic bacterial co-chaperonin GroES can be related not only to the fact that bacterial infection is a contributory factor to inflammation, but also suggests the potential role of bacterial infection in the initiating of the amyloid depositions via seeding [82].

As a result, a self-perpetuating cycle can be triggered in the ageing prostate, leading ultimately to amyloid growth. The increasing concentration of aggregation-prone

proteins in the sites of inflammation would favour their amyloid assembly and deposition, as amyloid formation is a concentration-dependent process. This can be further promoted by the presence of calcium and zinc salts abundant in corpora amylacea and S100A8/A9 in turn can themselves regulate their own calcification. In the course of corpora amylacea growth, neighbouring acini are obstructed, exacerbating inflammation and enhancing the risk of neoplastic transformation. Thus, the direct involvement of proinflammatory S100A8/A9 proteins in corpora amylacea biogenesis emphasizes their role in the age-dependent prostate remodelling and accompanied ailments.

Amyloidogenic potential of S100 proteins

The amyloidogenic potential of a protein can be estimated using different algorithms that compute the aggregation and fibrillation propensity of a particular sequence. This approach was carried out using the ZYGGREGATOR algorithm to calculate the intrinsic aggregation propensity scores of monomeric S100A8 and S100A9 at pH 7.0 and 2.0, the conditions of their *in vitro* amyloid formation [14] (for a recent review, see [83]). The results evidenced a rather high propensity, comparable with that of Aβ peptides, forming amyloid deposits in Alzheimer's disease. The overall aggregation scores for S100A8 are 0.76 at pH 7.0 and 0.77 at pH 2.0; for S100A9, 1.04 and 0.65, and for $A\beta_{(1–40)}$ and $A\beta_{(1–42)}$ peptides at pH 7.0, 0.97 and 0.94, respectively. In both proteins, the Ca^{2+}-binding sites with low affinity (amino acid residues 20–33 for S100A8 and 23–36 for S100A9) and high affinity (amino acid residues 59–70 for S100A8 and 67–78 for S100A9) are located in close proximity to the segments that are highly aggregation prone. In the S100A8/A9 oligomeric complex, however, the amyloid scores for S100A8 and S100A9 are significantly reduced and equal to 0.18 and 0.32, respectively, indicating that most of the aggregation-prone sequences are involved in native complex formation. Therefore, we surmise that calcium-dependent native complex formation can effectively compete under physiological conditions with the calcium-dependent amyloid assembly, the latter possibly being prevalent in a destabilizing environment, leading to protein partial unfolding and native complex dissociation.

Building on these initial observations, and considering the fact that S100 proteins share a rather high chemical and structural identity, we further addressed the hypothesis that amyloid formation could be a generalized property among the members of the S100 protein family. For this purpose, we have carried out a series of preliminary experiments in conditions identical to those assayed for S100A8/A9 (pH 2 and 57 °C [14]), to test if other S100 proteins (S100A3, S100A6, S100A12 and S100B) would form thioflavin-T (ThT)-reactive amyloid species (H.M. Botelho, K. Yanamandra, G. Fritz, L.A. Morozova-Roche, C.M. Gomes, manuscript in preparation). Upon incubation for 50 h, three of the tested S100 proteins formed ThT-binding amyloid structures that resulted in an increase in fluorescence intensity of ThT, comparable with that observed upon dye interaction with the lysozyme amyloids used as a positive control (Fig. 3A). Only S100A12 did not yield ThT-reactive species under the tested conditions. The presence of amyloid and other precursor structures (fibres, protofibrils and disordered aggregates) was indentified using atomic force micros-

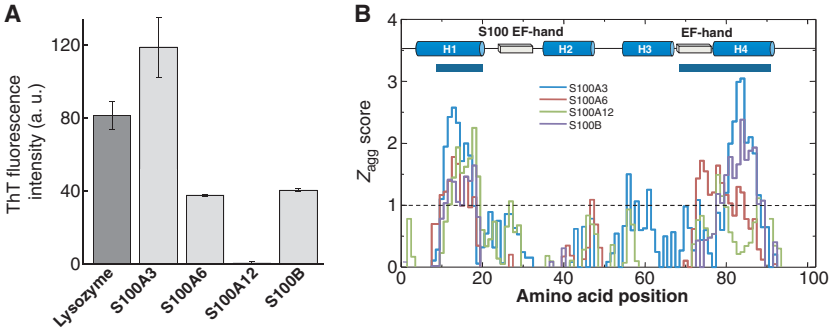

Fig. 3. Amyloidogenic potential of S100 proteins. (A) ThT fluorescence (482 nm) of S100 proteins (3 mg·mL^{-1}) after ~ 2 days incubation at pH 2.5, 57 °C without agitation and the positive control of lysozyme amyloid (10 mg·mL^{-1}) after ~ 8 days. Values are mean ± standard deviation. (B) *In silico* analysis of aggregation and amyloid formation propensities of selected S100 proteins. The top picture illustrates the location of consensus S100 motifs, the thick horizontal lines indicate the regions with high (> 95%) WALTZ score and the plot represents the position-dependent ZYGGREGATOR score. The horizontal dashed line indicates the significance threshold, the higher scores being significant. The amino acid position numbering is obtained after sequence alignment.

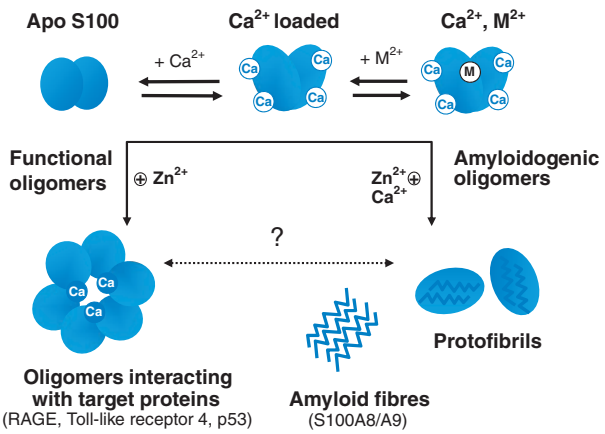

Fig. 4. Native states and oligomerization pathways in S100 proteins. A scheme outlining interconversion pathways of S100 proteins, evidencing Ca^{2+} and other metal (M^{2+}) binding sites, and possible routes for oligomerization pathways.

copy (data not shown). A complementary *in silico* analysis of the aggregation propensities and amyloid-forming sequences at pH 7 was also carried out using ZYGGREGATOR [83,84] and WALTZ [85] prediction tools, respectively. The results obtained with WALTZ (Fig. 3B, top) indicate that S100 proteins always contain amyloidogenic segments within helices H_I or H_{IV}, or in both helices. The aggregation propensity analysis using the ZYGGREGATOR algorithm allowed the propensity for the formation of β-rich oligomers (Z_{tox}) to be discriminated from the formation of fibrillar aggregates (Z_{agg}). The results of this analysis applied to the assayed S100 proteins revealed a similar high propensity clustering at helices H_I and H_{IV}, although with somewhat lower absolute values.

Together, these findings suggest that amyloid-like conformations (β-rich oligomers, protofibrils and fibres) might be accessible to S100 proteins under particular physiological conditions, and clearly metal ions play a determinant role in the process (Fig. 4). It is already established that Ca^{2+}, Zn^{2+} and Cu^{2+} promote conformational changes within the S100 fold that have an impact on protein stability (as in S100A2), on the formation of functional oligomers (as in S100B) and on the formation of amyloid fibres (as in S100A8/A9). Considering the latent propensity encoded in the primary sequence of S100 proteins to form β-rich oligomers and fibres, it is reasonable to envisage that factors such as an imbalance in metal homeostasis and anomalous protein–metal interactions, inflammation, oxidative stress or/and genetic mutations may provide conditions in the cellular milieu that affect any of the functional states of S100 proteins (Fig. 4) and result in the formation of amyloid structures or of its precursor oligomers in a physiological context. One interesting aspect that remains to be addressed and may even suggest a toxic gain of function characteristic to amyloid oligomers in general [86], is if S100 amyloids exacerbate the apoptoptic activity of the S100A8/A9 complex [74–76] or interact with the RAGE receptors, further contributing or abrogating the toxic effects. The latter are already known to be involved in Aβ peptide amyloid transport and recognition processes in the context of Alzheimer's disease. A contrasting perspective can also be hypothesized: considering that most of the S100 proteins have upregulated expression patterns in inflammatory, neurodegenerative and malignant proliferation processes, could amyloid formation serve as a sink for dangerous or somehow harmful proteins promoting inflammation or involved in cancer? Now that even Aβ plaques are viewed from a positive side [87], is it possible that the amyloid formation of S100 proteins may potentially play some 'positive' role? Future research in the coming years will certainly contribute to clarify some of these and other questions and will ultimately bring us to a higher level of understanding the biology of tumour and degeneration and enable to use our acquired knowledge of S100 structure and functions in developing strategies to modulate their activity for therapeutic purposes.

Acknowledgements

The work described in this review was supported by grants POCTI/QUI/45758 and PTDC/QUI/70101 (to CMG) from the Fundação para a Ciência e a Tecnologia (FCT/MCTES, Portugal), by grants FR 1488/3-1 and FR 1488/3-1 from the Deutsche Forschungsgemeinschaft (DFG) (to GF). CMG and GF are recipients of a CRUP/DAAD collaborative grant A-15/08. HMB is a recipient of a PhD fellowship (SFRH/BD/31126/2006) from Fundação para a Ciência e a Tecnologia (FCT/MCTES, Portugal). LMR research is supported by the Swedish Medical Research Council, Kempe Foundation, Brain Foundation and Insamlingsstiftelsen Sweden.

References

1 Moore BW (1965) A soluble protein characteristic of the nervous system. *Biochem Biophys Res Commun* **19**, 739–744.
2 Engelkamp D, Schäfer BW, Mattei MG, Erne P & Heizmann CW (1993) Six S100 genes are clustered on human chromosome 1q21: identification of two genes coding for the two previously unreported

calcium-binding proteins S100D and S100E. *Proc Natl Acad Sci USA* **90**, 6547–6551.
3 Schäfer BW, Wicki R, Engelkamp D, Mattei MG & Heizmann CW (1995) Isolation of a YAC clone covering a cluster of nine S100 genes on human chromosome 1q21: rationale for a new nomenclature of the S100 calcium-binding protein family. *Genomics* **25**, 638–643.
4 Salama I, Malone PS, Mihaimeed F & Jones JL (2008) A review of the S100 proteins in cancer. *Eur J Surg Oncol* **34**, 357–364.
5 Boom A, Pochet R, Authelet M, Pradier L, Borghgraef P, Van Leuven F, Heizmann CW & Brion JP (2004) Astrocytic calcium/zinc binding protein S100A6 over expression in Alzheimer's disease and in PS1/APP transgenic mice models. *Biochim Biophys Acta* **1742**, 161–168.
6 Mrak RE & Griffinbc WS (2001) The role of activated astrocytes and of the neurotrophic cytokine S100B in the pathogenesis of Alzheimer's disease. *Neurobiol Aging* **22**, 915–922.
7 Botelho HM, Koch M, Fritz G & Gomes CM (2009) Metal ions modulate the folding and stability of the tumor suppressor protein S100A2. *FEBS J* **276**, 1776–1786.
8 Heizmann CW & Cox JA (1998) New perspectives on S100 proteins: a multi-functional Ca(2+)-, Zn(2+)- and Cu(2+)-binding protein family. *Biometals* **11**, 383–397.
9 Bjork P, Bjork A, Vogl T, Stenstrom M, Liberg D, Olsson A, Roth J, Ivars F & Leanderson T (2009) Identification of human S100A9 as a novel target for treatment of autoimmune disease via binding to quinoline-3-carboxamides. *PLoS Biol* **7**, e97.
10 Leclerc E, Fritz G, Vetter SW & Heizmann CW (2009) Binding of S100 proteins to RAGE: an update. *Biochim Biophys Acta* **1793**, 993–1007.
11 Ostendorp T, Leclerc E, Galichet A, Koch M, Demling N, Weigle B, Heizmann CW, Kroneck PM & Fritz G (2007) Structural and functional insights into RAGE activation by multimeric S100B. *EMBO J* **26**, 3868–3878.
12 Donato R (2007) RAGE: a single receptor for several ligands and different cellular responses: the case of certain S100 proteins. *Curr Mol Med* **7**, 711–724.
13 Vogl T, Tenbrock K, Ludwig S, Leukert N, Ehrhardt C, van Zoelen MA, Nacken W, Foell D, van der Poll T, Sorg C *et al.* (2007) Mrp8 and Mrp14 are endogenous activators of Toll-like receptor 4, promoting lethal, endotoxin-induced shock. *Nat Med* **13**, 1042–1049.
14 Yanamandra K, Alexeyev O, Zamotin V, Srivastava V, Shchukarev A, Brorsson AC, Tartaglia GG, Vogl T, Kayed R, Wingsle G *et al.* (2009) Amyloid formation by the pro-inflammatory S100A8/A9 proteins in the ageing prostate. *PLoS ONE* **4**, e5562.
15 Koch M, Bhattacharya S, Kehl T, Gimona M, Vasak M, Chazin W, Heizmann CW, Kroneck PM & Fritz G (2007) Implications on zinc binding to S100A2. *Biochim Biophys Acta* **1773**, 457–470.
16 Korndörfer IP, Brueckner F & Skerra A (2007) The crystal structure of the human (S100A8/S100A9)2 heterotetramer, calprotectin, illustrates how conformational changes of interacting alpha-helices can determine specific association of two EF-hand proteins. *J Mol Biol* **370**, 887–898.
17 Moroz OV, Blagova EV, Wilkinson AJ, Wilson KS & Bronstein IB (2009) The crystal structures of human S100A12 in apo form and in complex with zinc: new insights into S100A12 oligomerisation. *J Mol Biol* **391**, 536–551.
18 Moroz OV, Antson AA, Dodson EJ, Burrell HJ, Grist SJ, Lloyd RM, Maitland NJ, Dodson GG, Wilson KS, Lukanidin E *et al.* (2002) The structure of S100A12 in a hexameric form and its proposed role in receptor signalling. *Acta Crystallogr D Biol Crystallogr* **58**, 407–413.
19 Marlatt NM, Boys BL, Konermann L & Shaw GS (2009) Formation of monomeric S100B and S100A11 proteins at low ionic strength. *Biochemistry* **48**, 1954–1963.
20 Santamaria-Kisiel L, Rintala-Dempsey AC & Shaw GS (2006) Calcium-dependent and -independent interactions of the S100 protein family. *Biochem J* **396**, 201–214.
21 Hunter MJ & Chazin WJ (1998) High level expression and dimer characterization of the S100 EF-hand proteins, migration inhibitory factor-related proteins 8 and 14. *J Biol Chem* **273**, 12427–12435.
22 Nacken W & Kerkhoff C (2007) The hetero-oligomeric complex of the S100A8/S100A9 protein is extremely protease resistant. *FEBS Lett* **581**, 5127–5130.
23 Vogl T, Leukert N, Barczyk K, Strupat K & Roth J (2006) Biophysical characterization of S100A8 and S100A9 in the absence and presence of bivalent cations. *Biochim Biophys Acta* **1763**, 1298–1306.
24 Baudier J, Mandel P & Gerard D (1983) Bovine brain S100 proteins: separation and characterization of a new S100 protein species. *J Neurochem* **40**, 145–152.
25 Yang Q, O'Hanlon D, Heizmann CW & Marks A (1999) Demonstration of heterodimer formation between S100B and S100A6 in the yeast two-hybrid system and human melanoma. *Exp Cell Res* **246**, 501–509.
26 Deloulme JC, Assard N, Mbele GO, Mangin C, Kuwano R & Baudier J (2000) S100A6 and S100A11 are specific targets of the calcium- and zinc-binding S100B protein *in vivo*. *J Biol Chem* **275**, 35302–35310.
27 Wang G, Rudland PS, White MR & Barraclough R (2000) Interaction *in vivo* and *in vitro* of the metastasis-inducing S100 protein, S100A4 (p9Ka) with S100A1. *J Biol Chem* **275**, 11141–11146.
28 Wang G, Zhang S, Fernig DG, Spiller D, Martin-Fernandez M, Zhang H, Ding Y, Rao Z, Rudland PS

& Barraclough R (2004) Heterodimeric interaction and interfaces of S100A1 and S100P. *Biochem J* **382**, 375–383.
29 Lehmann R, Melle C, Escher N & von Eggeling F (2005) Detection and identification of protein interactions of S100 proteins by ProteinChip technology. *J Proteome Res* **4**, 1717–1721.
30 Vogl T, Roth J, Sorg C, Hillenkamp F & Strupat K (1999) Calcium-induced noncovalently linked tetramers of MRP8 and MRP14 detected by ultraviolet matrix-assisted laser desorption/ionization mass spectrometry. *J Am Soc Mass Spectrom* **10**, 1124–1130. doi: S1044-0305(99)00085-9 [pii].
31 Novitskaya V, Grigorian M, Kriajevska M, Tarabykina S, Bronstein I, Berezin V, Bock E & Lukanidin E (2000) Oligomeric forms of the metastasis-related Mts1 (S100A4) protein stimulate neuronal differentiation in cultures of rat hippocampal neurons. *J Biol Chem* **275**, 41278–41286. doi: 10.1074/jbc.M007058200 [pii].
32 Rezvanpour A, Phillips JM & Shaw GS (2009) Design of high-affinity S100-target hybrid proteins. *Protein Sci* **18**, 2528–2536.
33 Brodersen DE, Nyborg J & Kjeldgaard M (1999) Zinc-binding site of an S100 protein revealed. Two crystal structures of Ca^{2+}-bound human psoriasin (S100A7) in the Zn^{2+}-loaded and Zn^{2+}-free states. *Biochemistry* **38**, 1695–1704.
34 Charpentier TH, Wilder PT, Liriano MA, Varney KM, Pozharski E, MacKerell AD Jr, Coop A, Toth EA & Weber DJ (2008) Divalent metal ion complexes of S100B in the absence and presence of pentamidine. *J Mol Biol* **382**, 56–73. doi: S0022-2836(08)00763-8 [pii] 10.1016/j.jmb.2008.06.047.
35 Koch M, Diez J & Fritz G (2008) Crystal structure of Ca^{2+}-free S100A2 at 1.6 A resolution. *J Mol Biol* **378**, 933–942.
36 Glaser R, Harder J, Lange H, Bartels J, Christophers E & Schroder JM (2005) Antimicrobial psoriasin (S100A7) protects human skin from Escherichia coli infection. *Nat Immunol* **6**, 57–64.
37 Baudier J, Glasser N & Gerard D (1986) Ions binding to S100 proteins. I. Calcium- and zinc-binding properties of bovine brain S100 alpha alpha, S100a (alpha beta), and S100b (beta beta) protein: Zn^{2+} regulates Ca^{2+} binding on S100b protein. *J Biol Chem* **261**, 8192–8203.
38 Dell'Angelica EC, Schleicher CH & Santome JA (1994) Primary structure and binding properties of calgranulin C, a novel S100-like calcium-binding protein from pig granulocytes. *J Biol Chem* **269**, 28929–28936.
39 Kerkhoff C, Vogl T, Nacken W, Sopalla C & Sorg C (1999) Zinc binding reverses the calcium-induced arachidonic acid-binding capacity of the S100A8/A9 protein complex. *FEBS Lett* **460**, 134–138.
40 Moroz OV, Burkitt W, Wittkowski H, He W, Ianoul A, Novitskaya V, Xie J, Polyakova O, Lednev IK, Shekhtman A *et al.* (2009) Both Ca^{2+} and Zn^{2+} are essential for S100A12 protein oligomerization and function. *BMC Biochem* **10**, 11.
41 Baudier J & Cole RD (1988) Interactions between the microtubule-associated tau proteins and S100b regulate tau phosphorylation by the Ca2+/calmodulin-dependent protein kinase II. *J Biol Chem* **263**, 5876–5883.
42 Yu WH & Fraser PE (2001) S100beta interaction with tau is promoted by zinc and inhibited by hyperphosphorylation in Alzheimer's disease. *J Neurosci* **21**, 2240–2246.
43 Mbele GO, Deloulme JC, Gentil BJ, Delphin C, Ferro M, Garin J, Takahashi M & Baudier J (2002) The zinc- and calcium-binding S100B interacts and co-localizes with IQGAP1 during dynamic rearrangement of cell membranes. *J Biol Chem* **277**, 49998–50007.
44 Gentil BJ, Delphin C, Mbele GO, Deloulme JC, Ferro M, Garin J & Baudier J (2001) The giant protein AHNAK is a specific target for the calcium- and zinc-binding S100B protein: potential implications for Ca2+ homeostasis regulation by S100B. *J Biol Chem* **276**, 23253–23261.
45 Barber KR, McClintock KA, Jamieson GA Jr, Dimlich RV & Shaw GS (1999) Specificity and Zn^{2+} enhancement of the S100B binding epitope TRTK-12. *J Biol Chem* **274**, 1502–1508.
46 Ionescu JG, Novotny J, Stejskal V, Latsch A, Blaurock-Busch E & Eisenmann-Klein M (2006) Increased levels of transition metals in breast cancer tissue. *Neuro Endocrinol Lett* **27**(Suppl. 1), 36–39.
47 Li M, Zhang Y, Liu Z, Bharadwaj U, Wang H, Wang X, Zhang S, Liuzzi JP, Chang SM, Cousins RJ *et al.* (2007) Aberrant expression of zinc transporter ZIP4 (SLC39A4) significantly contributes to human pancreatic cancer pathogenesis and progression. *Proc Natl Acad Sci USA* **104**, 18636–18641.
48 Nishikawa T, Lee IS, Shiraishi N, Ishikawa T, Ohta Y & Nishikimi M (1997) Identification of S100b protein as copper-binding protein and its suppression of copper-induced cell damage. *J Biol Chem* **272**, 23037–23041.
49 Schafer BW, Fritschy JM, Murmann P, Troxler H, Durussel I, Heizmann CW & Cox JA (2000) Brain S100A5 is a novel calcium-, zinc-, and copper ion-binding protein of the EF-hand superfamily. *J Biol Chem* **275**, 30623–30630. doi: 10.1074/jbc.M002260200 [pii].
50 Moroz OV, Antson AA, Grist SJ, Maitland NJ, Dodson GG, Wilson KS, Lukanidin E & Bronstein IB (2003) Structure of the human S100A12–copper complex: implications for host-parasite defence. *Acta Crystallogr D Biol Crystallogr* **59**, 859–867.
51 Landriscina M, Bagala C, Mandinova A, Soldi R, Micucci I, Bellum S, Prudovsky I & Maciag T (2001)

Copper induces the assembly of a multiprotein aggregate implicated in the release of fibroblast growth factor 1 in response to stress. *J Biol Chem* **276**, 25549–25557. doi: 10.1074/jbc.M102925200 [pii].
52 Xie J, Burz DS, He W, Bronstein IB, Lednev I & Shekhtman A (2007) Hexameric calgranulin C (S100A12) binds to the receptor for advanced glycated end products (RAGE) using symmetric hydrophobic target-binding patches. *J Biol Chem* **282**, 4218–4231.
53 Kiryushko D, Novitskaya V, Soroka V, Klingelhofer J, Lukanidin E, Berezin V & Bock E (2006) Molecular mechanisms of Ca(2+) signaling in neurons induced by the S100A4 protein. *Mol Cell Biol* **26**, 3625–3638.
54 Mossberg A, Mok KH, Morozova-Roche LA & Svanborg C (2010) Structure and function of human α-lactalbumin made lethal to tumor cells (HAMLET)-type complexes. *FEBS J* **277**, 4614–4625.
55 Zimmer DB & Van Eldik LJ (1986) Identification of a molecular target for the calcium-modulated protein S100. Fructose-1,6-bisphosphate aldolase. *J Biol Chem* **261**, 11424–11428.
56 Brozzi F, Arcuri C, Giambanco I & Donato R (2009) S100B protein regulates astrocyte shape and migration via interaction with Src kinase: implications for astrocyte development, activation, and tumor growth. *J Biol Chem* **284**, 8797–8811.
57 Millward TA, Heizmann CW, Schafer BW & Hemmings BA (1998) Calcium regulation of Ndr protein kinase mediated by S100 calcium-binding proteins. *EMBO J* **17**, 5913–5922.
58 Garbuglia M, Verzini M, Rustandi RR, Osterloh D, Weber DJ, Gerke V & Donato R (1999) Role of the C-terminal extension in the interaction of S100A1 with GFAP, tubulin, the S100A1- and S100B-inhibitory peptide, TRTK-12, and a peptide derived from p53, and the S100A1 inhibitory effect on GFAP polymerization. *Biochem Biophys Res Commun* **254**, 36–41.
59 Donato R (1987) Quantitative analysis of the interaction between S-100 proteins and brain tubulin. *Cell Calcium* **8**, 283–297.
60 Kilby PM, Van Eldik LJ & Roberts GC (1997) Identification of the binding site on S100B protein for the actin capping protein CapZ. *Protein Sci* **6**, 2494–2503.
61 Wright NT, Cannon BR, Wilder PT, Morgan MT, Varney KM, Zimmer DB & Weber DJ (2009) Solution structure of S100A1 bound to the CapZ peptide (TRTK12). *J Mol Biol* **386**, 1265–1277.
62 Austermann J, Nazmi AR, Heil A, Fritz G, Kolinski M, Filipek S & Gerke V (2009) Generation and characterization of a novel, permanently active S100P mutant. *Biochim Biophys Acta* **1793**, 1078–1085.
63 Koltzscher M, Neumann C, Konig S & Gerke V (2003) Ca2+-dependent binding and activation of dormant ezrin by dimeric S100P. *Mol Biol Cell* **14**, 2372–2384.
64 Baudier J, Delphin C, Grunwald D, Khochbin S & Lawrence JJ (1992) Characterization of the tumor suppressor protein p53 as a protein kinase C substrate and a S100b-binding protein. *Proc Natl Acad Sci USA* **89**, 11627–11631.
65 Mueller A, Schafer BW, Ferrari S, Weibel M, Makek M, Hochli M & Heizmann CW (2005) The calcium-binding protein S100A2 interacts with p53 and modulates its transcriptional activity. *J Biol Chem* **280**, 29186–29193.
66 Grigorian M, Andresen S, Tulchinsky E, Kriajevska M, Carlberg C, Kruse C, Cohn M, Ambartsumian N, Christensen A, Selivanova G *et al.* (2001) Tumor suppressor p53 protein is a new target for the metastasis-associated Mts1/S100A4 protein: functional consequences of their interaction. *J Biol Chem* **276**, 22699–22708.
67 Ehrchen JM, Sunderkotter C, Foell D, Vogl T & Roth J (2009) The endogenous Toll-like receptor 4 agonist S100A8/S100A9 (calprotectin) as innate amplifier of infection, autoimmunity, and cancer. *J Leukoc Biol* **86**, 557–566. doi: jlb.1008647 [pii] 10.1189/jlb.1008647.
68 Foell D, Wittkowski H, Vogl T & Roth J (2007) S100 proteins expressed in phagocytes: a novel group of damage-associated molecular pattern molecules. *J Leukoc Biol* **81**, 28–37. doi: jlb.0306170 [pii] 10.1189/jlb.0306170.
69 Loser K, Vogl T, Voskort M, Lueken A, Kupas V, Nacken W, Klenner L, Kuhn A, Foell D, Sorokin L *et al.* (2010) The Toll-like receptor 4 ligands Mrp8 and Mrp14 are crucial in the development of autoreactive CD8+ T cells. *Nat Med* **16**, 713–717. doi:10.1038/nm.2150.
70 Hiratsuka S, Watanabe A, Sakurai Y, Akashi-Takamura S, Ishibashi S, Miyake K, Shibuya M, Akira S, Aburatani H & Maru Y (2008) The S100A8-serum amyloid A3-TLR4 paracrine cascade establishes a pre-metastatic phase. *Nat Cell Biol* **10**, 1349–1355. doi: ncb1794 [pii] 10.1038/ncb1794.
71 Donato R, Sorci G, Riuzzi F, Arcuri C, Bianchi R, Brozzi F, Tubaro C & Giambanco I (2009) S100B's double life: intracellular regulator and extracellular signal. *Biochim Biophys Acta* **1793**, 1008–1022. doi: S0167-4889(08)00409-6 [pii] 10.1016/j.bbamcr.2008.11.009.
72 Businaro R, Leone S, Fabrizi C, Sorci G, Donato R, Lauro GM & Fumagalli L (2006) S100B protects LAN-5 neuroblastoma cells against Abeta amyloid-induced neurotoxicity via RAGE engagement at low doses but increases Abeta amyloid neurotoxicity at high doses. *J Neurosci Res* **83**, 897–906. doi: 10.1002/jnr.20785.
73 Turovskaya O, Foell D, Sinha P, Vogl T, Newlin R, Nayak J, Nguyen M, Olsson A, Nawroth PP, Bierhaus A *et al.* (2008) RAGE, carboxylated glycans and S100A8/A9 play essential roles in colitis-associated carcinogenesis. *carcinogenesis* **29**, 2035–2043. doi: bgn188 [pii] 10.1093/carcin/bgn188.

74 Ghavami S, Kerkhoff C, Chazin WJ, Kadkhoda K, Xiao W, Zuse A, Hashemi M, Eshraghi M, Schulze-Osthoff K, Klonisch T *et al*. (2008) S100A8/9 induces cell death via a novel, RAGE-independent pathway that involves selective release of Smac/DIABLO and Omi/HtrA2. *Biochim Biophys Acta* **1783**, 297–311. doi: S0167-4889(07)00248-0 [pii] 10.1016/j.bbamcr.2007.10.015.

75 Viemann D, Barczyk K, Vogl T, Fischer U, Sunderkotter C, Schulze-Osthoff K & Roth J (2007) MRP8/MRP14 impairs endothelial integrity and induces a caspase-dependent and -independent cell death program. *Blood* **109**, 2453–2460. doi: blood-2006-08-040444 [pii] 10.1182/blood-2006-08-040444.

76 Ghavami S, Eshragi M, Ande SR, Chazin WJ, Klonisch T, Halayko AJ, McNeill KD, Hashemi M, Kerkhoff C & Los M (2010) S100A8/A9 induces autophagy and apoptosis via ROS-mediated cross-talk between mitochondria and lysosomes that involves BNIP3. *Cell Res* **20**, 314–331. doi: cr2009129 [pii] 10.1038/cr.2009.129.

77 Cross PA, Bartley CJ & McClure J (1992) Amyloid in prostatic corpora amylacea. *J Clin Pathol* **45**, 894–897.

78 De Marzo AM, Platz EA, Sutcliffe S, Xu J, Gronberg H, Drake CG, Nakai Y, Isaacs WB & Nelson WG (2007) Inflammation in prostate carcinogenesis. *Nat Rev Cancer* **7**, 256–269.

79 McCormick MM, Rahimi F, Bobryshev YV, Gaus K, Zreiqat H, Cai H, Lord RS & Geczy CL (2005) S100A8 and S100A9 in human arterial wall. Implications for atherogenesis. *J Biol Chem* **280**, 41521–41529.

80 Kayed R, Head E, Sarsoza F, Saing T, Cotman CW, Necula M, Margol L, Wu J, Breydo L, Thompson JL *et al*. (2007) Fibril specific, conformation dependent antibodies recognize a generic epitope common to amyloid fibrils and fibrillar oligomers that is absent in prefibrillar oligomers. *Mol Neurodegener* **2**, 18.

81 Pedersen JS, Andersen CB & Otzen DE (2010) Amyloid structure – one but not the same: the many levels of fibrillar polymorphism. *FEBS J* **277**, 4591–4601.

82 Otzen D & Nielsen PH (2008) We find them here, we find them there: functional bacterial amyloid. *Cell Mol Life Sci* **65**, 910–927.

83 Tartaglia GG & Vendruscolo M (2008) The Zyggregator method for predicting protein aggregation propensities. *Chem Soc Rev* **37**, 1395–1401.

84 Tartaglia GG, Pawar AP, Campioni S, Dobson CM, Chiti F & Vendruscolo M (2008) Prediction of aggregation-prone regions in structured proteins. *J Mol Biol* **380**, 425–436.

85 Maurer-Stroh S, Debulpaep M, Kuemmerer N, de la Paz ML, Martins IC, Reumers J, Morris KL, Copland A, Serpell L, Serrano L *et al*. (2010) Exploring the sequence determinants of amyloid structure using position-specific scoring matrices. *Nat Methods* **7**, 237–242.

86 Stefani M (2010) Biochemical and biophysical features of both oligomer/fibril and cell membrane in amyloid cytotoxicity. *FEBS J* **277**, 4602–4613.

87 Heo C, Chang KA, Choi HS, Kim HS, Kim S, Liew H, Kim JA, Yu E, Ma J & Suh YH (2007) Effects of the monomeric, oligomeric, and fibrillar Abeta42 peptides on the proliferation and differentiation of adult neural stem cells from subventricular zone. *J Neurochem* **102**, 493–500. doi: JNC4499 [pii] 10.1111/j.1471-4159.2007.04499.x.